

OMP-Based Channel Estimation With Dynamic Grid for mmWave MIMO Positioning Systems

Ngoc-Son Duong^{ID}, Graduate Student Member, IEEE, Quoc-Tuan Nguyen, and Thai-Mai Dinh-Thi^{ID}

The co-authors dedicate this work to Prof. Quoc-Tuan Nguyen, who passed away after the submission of the paper.

Abstract—Location information would become more critical in next-generation networks. In this letter, we introduce a novel estimation method for location-related parameters, i.e., Time-of-Arrival (TOA), Angle-of-Departure (AOD), Angle-of-Arrival (AOA), and channel amplitude in mmWave MIMO systems. Because of the sparse nature of the mmWave channel, we first coarsely estimate all parameters using compressive sensing (CS). To mitigate the error caused by basis mismatch, we coordinately apply Golden-Section search for AOD and AOA, followed by instant estimates of channel amplitude and TOA using Least Square (LS) with only two up-to-date atoms of AOA and AOD, in descent manner. Finally, channel amplitude and TOA is re-estimated by CS with mismatch-free basis, which is obtained from refined atoms. Simulations show that the proposed method can approach the exact value of all parameters with faster convergence and lower algorithmic complexity than full-dimensional search based on Newton-Type algorithms.

Index Terms—5G positioning, mmWave, channel estimation, MIMO, golden-section search, OMP, TOA, AOD, AOA.

I. INTRODUCTION

NEW potentials are presented by mmWave communication systems for enhancing the reliability and quality of communications as well as for precise user equipment (UE) location from a single base station (BS) [3], [4]. Recent theoretical studies have demonstrated the possibility of positioning the UE and mapping the propagation environments simultaneously using the resolvable angle-of-departures (AODs), angle-of-arrivals (AOAs), and time of arrivals (TOAs) [1]. It discovered that, provided the BS and UE are synchronized, a UE could process signals from a single BS in order to (i) determine its own position and orientation and (ii) estimate the reflectors in the environment. Many methods have been proposed to estimate mmWave channels for both communication and positioning. The common method is to use compressive sensing (CS) to take advantage of the sparsity of mmWave channels [5]. Others also considered Bayesian learning [6]. Very recent work

uses atomic norm minimization [7] or tensor decomposition plus joint angle and delay estimation (JADE) algorithm to estimate mmWave channels. The author in [1] introduced an estimation method of UE's location and orientation that included three steps. Location is indirectly determined in the third step through location-related parameters, i.e., AOD, AOA, TOA, and channel gain in the first two steps. The first step utilizes distributed compressed sensing simultaneous orthogonal matching pursuit (DCS-SOMP) to estimate channel-related parameters coarsely. The second step uses space-alternating generalized expectation maximization (SAGE) to refine coarse parameters. The setting of SAGE can be viewed as coordinate descent optimization with a maximization step involving a Newton-type algorithm using derivatives of a cost function to single parameters. Hence, this method draws a high computation cost with slow convergence and is also quite impractical in choosing the descent coefficient.

In this letter, we rely on [1] and extend our work in [10] to propose a computationally efficient OMP-based method for off-grid estimation. The proposed method focuses on fine-tuning the four positioning parameters, i.e., AOD, AOA, TOA, and channel amplitude, of the mmWave MIMO systems. We first perform Golden-Section searches on AOA and AOD and then apply atomic-based LS to the channel coefficient to construct a mismatch-free basis. After that, TOA and channel gain are re-estimated using the basis found in the previous step. In this way, our algorithm provides high accuracy equivalent to a full Newton-Type-based search method while achieving two-time faster in terms of computation time.

Notation: Scalars are denoted in *italic*, e.g., x . Lower case boldface indicates a column vector, e.g., \mathbf{x} . Upper case boldface denotes a matrix, e.g., \mathbf{X} . Matrix transpose, conjugate transpose, and inverse are indicated by superscript \top , \mathbf{H} , and $^{-1}$, respectively. The Euclidean norm is denoted by $\|\cdot\|_2$ and set of complex numbers is denoted by \mathbb{C} .

II. MODELS AND PROBLEM DEFINITIONS

We consider the MIMO OFDM system with N subcarriers. The channel between a base station (BS) and a user equipment (UE) is multipath, which can be represented by the Saleh-Valenzuela model [11] with K individual physical scattering paths. BS and UE are equipped with ULA antenna with N_t and N_r antenna elements, respectively. Let $n = 0, 1, \dots, N-1$ be the sub-carrier index, the MIMO matrix channel can be written as:

$$\mathbf{H}(n) = \mathbf{A}_{R_x}[n]\mathbf{\Gamma}[n]\mathbf{A}_{T_x}[n]^\top \quad (1)$$

Manuscript received 28 April 2023; revised 30 June 2023; accepted 31 July 2023. Date of publication 9 August 2023; date of current version 11 October 2023. Ngoc-Son Duong was funded by Vingroup JSC and supported by the master's, Ph.D. Scholarship Program of Vingroup Innovation Foundation (VINIF), Institute of Big Data, code VINIF.2021.TS.094. The associate editor coordinating the review of this letter and approving it for publication was S. Bartoletti. (Corresponding author: Thai-Mai Dinh-Thi.)

The authors are with the Department of Telecommunications Systems, Faculty of Electronics and Telecommunications, Vietnam National University (VNU)—University of Engineering and Technology, Hanoi 100000, Vietnam (e-mail: sondn24@vnu.edu.vn; tuannq@vnu.edu.vn; dtmai@vnu.edu.vn).

Digital Object Identifier 10.1109/LCOMM.2023.3303453

1558-2558 © 2023 IEEE. Personal use is permitted, but republication/redistribution requires IEEE permission. See <https://www.ieee.org/publications/rights/index.html> for more information.

where, $\mathbf{A}_{\text{Tx}}[n] \in \mathbb{C}^{N_t \times K}$ and $\mathbf{A}_{\text{Rx}}[n] \in \mathbb{C}^{N_r \times K}$ are steering vector matrices of transmitted and received antenna, respectively. They are defined by:

$$\mathbf{A}_{\text{Tx}}[n] = [\mathbf{a}_{\text{Tx},n}(\theta_{\text{Tx},0}), \dots, \mathbf{a}_{\text{Tx},n}(\theta_{\text{Tx},K-1})]^\top \quad (2)$$

$$\mathbf{A}_{\text{Rx}}[n] = [\mathbf{a}_{\text{Rx},n}(\theta_{\text{Rx},0}), \dots, \mathbf{a}_{\text{Rx},n}(\theta_{\text{Rx},K-1})]^\top \quad (3)$$

For ULA, steering vector $\mathbf{a}_{\text{Tx},n} \in \mathbb{C}^{N_t}$ and $\mathbf{a}_{\text{Rx},n} \in \mathbb{C}^{N_r}$ correspond to k^{th} path are defined as:

$$\mathbf{a}_{\text{Tx},n}(\theta_{\text{Tx},k}) = [1, e^{-j\pi \sin(\theta_{\text{Tx},k})}, \dots, e^{-j\pi(N_t-1) \sin(\theta_{\text{Tx},k})}]^\top \quad (4)$$

$$\mathbf{a}_{\text{Rx},n}(\theta_{\text{Rx},k}) = [1, e^{-j\pi \sin(\theta_{\text{Rx},k})}, \dots, e^{-j\pi(N_r-1) \sin(\theta_{\text{Rx},k})}]^\top \quad (5)$$

The channel gain and path loss-related matrix $\Gamma[n]$ is defined as:

$$\Gamma[n] = \text{diag} \left(|\tilde{h}_0| e^{\frac{-j2\pi n \tau_0}{NT_s}}, \dots, |\tilde{h}_{K-1}| e^{\frac{-j2\pi n \tau_{K-1}}{NT_s}} \right) \quad (6)$$

where, \tilde{h}_k is the complex channel gain. The channel is considered to be constant during transmission. Assume that the BS transmit a pilot signal \mathbf{x} in the downlink to UE using a beamforming matrix $\mathbf{F}[n]$. The received signal can be written as:

$$\mathbf{y}^{(g)}[n] = \mathbf{H}[n]\mathbf{F}^{(g)}[n]\mathbf{x}^{(g)}[n] + \mathbf{n}^{(g)}[n] \quad (7)$$

where, the superscript (g) indicate for g^{th} transmission in a sequence of G signals and $\mathbf{n}^{(g)}[n]$ is the zero-mean Gaussian noise. Our problem is to estimate AOD, AOA, TOA and channel amplitude given $\mathbf{y}^{(g)}[n]$.

III. PROPOSED ESTIMATION METHOD

Let $\mathbf{U}_{\text{Tx}} \in \mathbb{C}^{N_t \times N_b}$ and $\mathbf{U}_{\text{Rx}} \in \mathbb{C}^{N_r \times N_b}$ are unitary transformation matrix that convert signal to angular domain and defined as:

$$\mathbf{U}_{\text{Tx}} \triangleq [\mathbf{u}_{\text{Tx}}(\bar{\omega}_1), \mathbf{u}_{\text{Tx}}(\bar{\omega}_2), \dots, \mathbf{u}_{\text{Tx}}(\bar{\omega}_{N_b})], \quad (8)$$

$$\mathbf{U}_{\text{Rx}} \triangleq [\mathbf{u}_{\text{Rx}}(\bar{\omega}_1), \mathbf{u}_{\text{Rx}}(\bar{\omega}_2), \dots, \mathbf{u}_{\text{Rx}}(\bar{\omega}_{N_b})], \quad (9)$$

where $\mathbf{u}_{\text{Tx}}(\bar{\omega}_i)$, $\mathbf{u}_{\text{Rx}}(\bar{\omega}_i)$ are called the atoms of \mathbf{U}_{Tx} and \mathbf{U}_{Rx} , respectively. The vectorized version of $\mu[n] = \mathbf{H}[n]\mathbf{F}^{(g)}[n]\mathbf{x}^{(g)}[n]$ can be written as:

$$\text{vec}(\mu[n]) = \left(\mathbf{U}_{\text{Tx}}^H \mathbf{F}^{(g)}[n] \mathbf{x}^{(g)}[n] \right)^\top \otimes \mathbf{U}_{\text{Rx}} \text{vec}(\mathbf{U}_{\text{Rx}}^H \mathbf{H}[n] \mathbf{U}_{\text{Tx}}) \quad (10)$$

The quantity $\check{\mathbf{H}}[n] = \mathbf{U}_{\text{Rx}}^H \mathbf{H}[n] \mathbf{U}_{\text{Tx}} \in \mathbb{C}^{N_b \times N_b}$ is called beamspace channel with N_b is number of virtual beam in beamspace. $\check{\mathbf{H}}[n]$ can be written as:

$$\check{\mathbf{H}}[n] = \sum_{k=0}^{K-1} \mathbf{U}_{\text{Rx}}^H \mathbf{a}_{\text{Rx},n}(\theta_{\text{Rx},k}) |\tilde{h}_k| e^{\frac{-j2\pi n \tau_k}{NT_s}} \mathbf{a}_{\text{Tx},n}^H(\theta_{\text{Tx},k}) \mathbf{U}_{\text{Tx}} \quad (11)$$

Let $\Omega[n] = \left(\mathbf{U}_{\text{Tx}}^H \mathbf{F}^{(g)}[n] \mathbf{x}^{(g)}[n] \right)^\top \otimes \mathbf{U}_{\text{Rx}}$ and $\check{\mathbf{h}}[n] = \text{vec}(\check{\mathbf{H}}[n])$, (7) can be expressed as:

$$\check{\mathbf{y}}[n] = \Omega[n] \check{\mathbf{h}}[n] + \check{\mathbf{n}}[n] \quad (12)$$

A. Coarse Estimation Using DCS-SOMP

Since the channel is characterized by very few paths, the representation of $\check{\mathbf{H}}[n] = \mathbf{U}_{\text{Rx}}^H \mathbf{H}[n] \mathbf{U}_{\text{Tx}}$ in the angular domain would be a sparse matrix with high-energy entries representing AOA and AOD. Herein, we choose DCS-SOMP for sparse recovery because of its accuracy and processing speed. From the found columns in $\Omega[n]$, we can coarsely estimate AOD, AOA, TOA, and channel gain via some mapping function as presented in [1]. The recovered channel can be written as:

$$\hat{\mathbf{H}}[n] = \sum_{k=0}^{K-1} |\hat{h}_k| e^{\frac{-j2\pi n \hat{\tau}_k}{NT_s}} f(\bar{\theta}_{\text{Rx},k}, \bar{\theta}_{\text{Tx},k}) \quad (13)$$

where, $f(\bar{\theta}_{\text{Rx},k}, \bar{\theta}_{\text{Tx},k})$ is defined as:

$$f(\bar{\theta}_{\text{Rx},k}, \bar{\theta}_{\text{Tx},k}) \triangleq \mathbf{u}_{\text{Rx}}^H(\bar{\theta}_{\text{Rx},k}) \mathbf{a}_{\text{Rx},n}(\bar{\theta}_{\text{Rx},k}) \mathbf{a}_{\text{Tx},n}^H(\bar{\theta}_{\text{Tx},k}) \mathbf{u}_{\text{Tx}}(\bar{\theta}_{\text{Tx},k}) \quad (14)$$

where, $\bar{\theta}_{\text{Rx},k}$ and $\bar{\theta}_{\text{Tx},k}$ are quantized AOA and AOD to nearest atom $\mathbf{u}_{\text{Rx}}^H(\bar{\theta}_{\text{Rx},k})$ and $\mathbf{u}_{\text{Tx}}^H(\bar{\theta}_{\text{Tx},k})$ of \mathbf{U}_{Rx} and \mathbf{U}_{Tx} , respectively.

B. Refinement Using Golden-Section Search and DSC-SOMP

1) *Loss Function*: We first define the loss function of our problem for all sub-carriers as:

$$\check{\mathbf{y}} = \text{vec}(\check{\mathbf{y}}[n]) = \sum_{k=0}^{K-1} (\check{\Omega} \check{\mathbf{h}}_k + \check{\mathbf{n}}_k) \quad (15)$$

where, $\check{\Omega} = \text{blkdiag}\{\Omega[0], \dots, \Omega[N-1]\}$. Let $\boldsymbol{\eta} = [\eta_0, \eta_1, \dots, \eta_{K-1}]^\top$ be the set of parameter associated with all path, where $\eta_k = [\theta_{\text{Tx},k}, \theta_{\text{Rx},k}, \tau_k, |\tilde{h}_k|]^\top$. Let $\hat{\eta}^{(i)}$ be the estimate of $\boldsymbol{\eta}$ at i^{th} step. The loss function related to k^{th} path should be:

$$Q(\eta_k | \hat{\eta}^{(i)}) = \|\check{\mathbf{y}} - \sum_{l \neq k, l=0}^{K-1} \check{\Omega} \hat{\mathbf{h}}_l^{(i)} - \check{\Omega} \check{\mathbf{h}}_k\|_2^2 \quad (16)$$

It should be noted that when we write as (16), we want to estimate the channel for each path in coordinate descent manner.

2) *Optimize Object Function*: In this step, the main task is to find η_k so that (16) reach minimum, in other words:

$$\hat{\eta}_k^{(i+1)} = \arg \min_{\eta_k} Q(\eta_k | \hat{\eta}^{(i)}) \quad (17)$$

One can sequentially update all parameters using a Newton-Type algorithm (see Appendix). We, instead, use the Golden-Section search as another option for minimization to avoid slow convergence rate and the impractical of choosing the descent coefficient for all parameters. This would draw a 4D search over four channel parameters. Hence, we herein propose a lighter search method compared to conventional one. Taking OMP into re-consideration, it would be optimal if it does not suffer from the off-grid effect. So, it is reasonable to acquire a sensing matrix that avoids this effect. From (17), we can see that only $\check{\Omega}$ contains information about AOA and AOD. If we do not care about channel amplitude and TOA, we can update AOA and AOD using Golden-Section search and LS for channel coefficient, following coordinate descent

manner. In this way, LS ensures that (17) is minimized while AOA and AOD approach their exact values in continuous domain. However, inverting big matrix $\tilde{\Omega}$ requires a lot of computer resources. As a result, using LS to directly estimate the channel coefficient $\hat{\mathbf{h}}_k$ is impractical. Realizing that the basis is completely unchanged during the estimation process except for the atoms index that are related to AOA and AOD, we only use AOA and AOD found in each step to construct a new basis as follows:

$$\tilde{\omega}^{(i)}[n] \triangleq \left(\mathbf{u}_{\text{Tx}}^H(\hat{\theta}_{\text{Tx},k}^{(i)}) \mathbf{F}^{(g)}[n] \mathbf{x}^{(g)}[n] \right)^\top \otimes \mathbf{u}_{\text{Rx}}(\hat{\theta}_{\text{Rx},k}^{(i)}) \quad (18)$$

$\mathbf{u}_{\text{Rx}}(\hat{\theta}_{\text{Rx},k}^{(i)})$ can be defined as:

$$\mathbf{u}_{\text{Rx}}(\hat{\theta}_{\text{Rx},k}^{(i)}) = \left[1, e^{-j\pi \sin(\hat{\theta}_{\text{Rx},k}^{(i)})}, \dots, e^{-j\pi(N-1) \sin(\hat{\theta}_{\text{Rx},k}^{(i)})} \right]^\top \quad (19)$$

$\mathbf{u}_{\text{Tx}}(\hat{\theta}_{\text{Tx},k}^{(i)})$ is defined the same by replacing subscript Rx by Tx. By this way, we reduce the size of $\tilde{\Omega}$ from $N_r N_s N \times N_b N_b N$ to $N_r N_s N \times N$ and easy to estimate channel coefficient, $\hat{\mathbf{h}}_k^{(i)} = [\hat{h}_k^{(i)}[0], \hat{h}_k^{(i)}[1], \dots, \hat{h}_k^{(i)}[N-1]]^\top$, by LS:

$$\hat{\mathbf{h}}_k^{(i)} = \left(\left(\omega^{(i)} \right)^\text{H} \omega^{(i)} \right)^{-1} \left(\tilde{\omega}^{(i)} \right)^\text{H} \left(\tilde{\mathbf{y}} - \sum_{l \neq k, l=0}^K \tilde{\omega} \hat{\mathbf{h}}_l^{(i)} \right) \quad (20)$$

Unfortunately, the channel amplitude and TOA that are extracted from the channel coefficient do not approach their correct values since they are estimated by an incomplete basis. Hence, only AOA and AOD are correctly estimated at the end of the refinement step. However, correct AOA and AOD are the foundation of a mismatch-free basis. Hence, we re-update the original sensing matrix by replacing atoms found at the initial step with *refined* atoms and directly estimate the channel coefficient using DSC-SOMP to have a better estimator of channel amplitude and TOA. By doing this, the index of the atom found by DSC-SOMP in the initial step and the last step is the same. Fig. 1 illustrates how our method works. In Fig. 1, the red and blue circles denote the quantized and true values of AOD and AOA, respectively. The red grids represent atoms that are related to the instant AOD and AOA estimates. Since AOA and AOD change during the refinement process, these red grids are dynamically updated. Meanwhile, the black grids denote atoms that do not change over time. The proposed channel estimation method is given by Algorithm 1. After having AOA, AOD, TOA and channel amplitude for all paths, we use a weighted LS, which is proposed in [9], to convert them to UE's position and orientation.

IV. SIMULATION RESULTS AND DISCUSSION

We take into account both the LOS and NLOS propagation channels between the BS and UE in the 2D Cartesian coordinate system. We choose 60 GHz for the central frequency, 100 MHz for the bandwidth, 3×10^8 m/s for the light speed, and 10 for the number of sub-carriers. In both the transmitter and the receiver, the number of antenna elements is

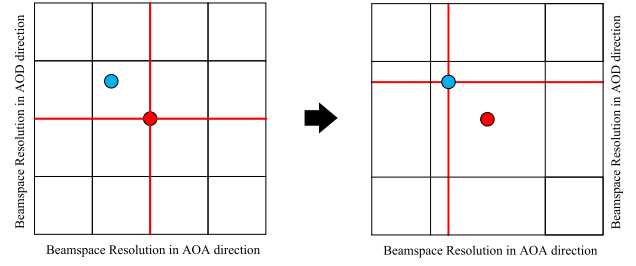


Fig. 1. The basis changes from off-grid to on grid.

Algorithm 1 Proposed Refinement Method for mmWave Channel Estimation

Input: Received Signal: $\tilde{\mathbf{y}}$; Sensing matrix: $\tilde{\Omega}$; Max iter: M , Number of path: K ; Coarse parameter: $\hat{\eta}^{(0)}$; Coarse channel: $\hat{\mathbf{h}}_k^{(0)}$

Output: $\hat{\eta}^{(M+1)}$

$\hat{\mathbf{H}}^{(0)} = \text{reshape}(\hat{\mathbf{h}}^{(0)}, [N_b \times N_b])$;

for $k = 0 \rightarrow K - 1$ **do**

$[r_k, c_k] = \text{find}(|\hat{\mathbf{H}}^{(0)}| \neq 0)$;

end

// Refinement using Golden-Section search;

for $i = 1, \dots, M$ **do**

 Coordinateally evaluate: $\tilde{\mathbf{y}} - \sum_{l \neq k, l=0}^K \tilde{\omega} \hat{\mathbf{h}}_l^{(i)}$;

for $k = 0, \dots, K - 1$ **do**

$\hat{\theta}_{\text{Tx},k}^{(i)} = \text{GOLDEN SEARCH}(\hat{\theta}_{\text{Tx},k}^{(i-1)}, \tilde{\Omega})$;

$\hat{\theta}_{\text{Rx},k}^{(i)} = \text{GOLDEN SEARCH}(\hat{\theta}_{\text{Rx},k}^{(i-1)}, \tilde{\Omega})$;

 Construct new basis using (18);

 Evaluate (20) to minimize (16);

$|\hat{h}_k^{(i)}| = \frac{1}{N} |\hat{\mathbf{h}}_k^{(i)}|$; $\hat{\tau}_k^{(i)} = -\frac{1}{N} \left(\angle(\hat{\mathbf{h}}_k^{(i)}) \right) \times \frac{NT_s}{2\pi}$;

end

end

// Re-update sensing matrix;

for $k = 0, \dots, K - 1$ **do**

$\mathbf{U}_{\text{Tx}}(:, c_k) = \mathbf{u}_{\text{Tx}}(\hat{\theta}_{\text{Tx},k}^{(M)})$;

$\mathbf{U}_{\text{Rx}}(:, r_k) = \mathbf{u}_{\text{Rx}}(\hat{\theta}_{\text{Rx},k}^{(M)})$;

end

$\Omega[n] = \left(\mathbf{U}_{\text{Tx}}^H \mathbf{F}^{(g)}[n] \mathbf{x}^{(g)}[n] \right)^\top \otimes \mathbf{U}_{\text{Rx}}$;

$\tilde{\Omega} = \text{blkdiag}\{\Omega[0], \dots, \Omega[N-1]\}$;

// Re-estimate channel using new sensing matrix;

$\hat{\mathbf{h}}^{(M+1)} = \text{DCS-SOMP}(\tilde{\mathbf{y}}, \tilde{\Omega}, K)$;

for $k = 0, \dots, K - 1$ **do**

$|\hat{h}_k^{(M+1)}| = \frac{1}{N} |\hat{\mathbf{h}}_k^{(M+1)}|$;

$\hat{\tau}_k^{(M+1)} = -\frac{1}{N} \left(\angle(\hat{\mathbf{h}}_k^{(M+1)}) \right) \times \frac{NT_s}{2\pi}$;

end

specified to be 32. The BS is at a known position $\mathbf{q} = [0, 0]^\top$. The UE position and scatter are unknown and located at $\mathbf{p} = [4, 0]^\top$, $\mathbf{s} = [2, 2]^\top$, respectively. For the sake of simplicity, the channel statistic for LOS and NLOS is the same, and the loss is simply dependent on distance. The method using the

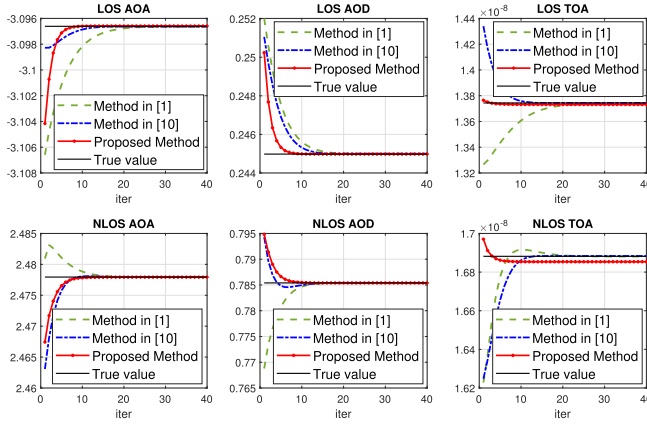


Fig. 2. At the end of the refinement step of a typical run at a high SNR level.

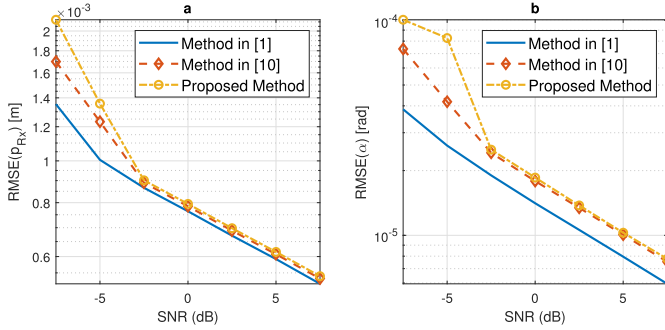


Fig. 3. Root mean squared error (RMSE) for *a*) position and *b*) rotation error in dB scale of the proposed algorithm versus traditional ones.

Newton-Type algorithm [1] for the refinement step is selected as a benchmark. The algorithmic complexity and accuracy of the estimated target's location and orientation are performance factors for comparison.

A. On the Accuracy and Convergence

Fig. 2 shows how parameters converge at the end of the refinement step. We see that all of the parameters, regardless of method, move downward from their coarse to convergent values. All three methods have similar accuracy in terms of AOA and AOD. However, the TOA of the proposed method does not converge to the exact value. The reason is that TOA is only estimated by incomplete basis ($\tilde{\omega}[n]$). The period of relative stability of our method can be reached after 6–8 iterations. Meanwhile, the methods of only using Golden-Section search and the Newton method converge at rates of 10 and 20 iterations, respectively. Fig. 3 shows the position and orientation errors of three methods versus SNR. As we can see, the accuracy of both indicators increases with SNR. The proposed method has similar performance and is close to the accuracy of the Newton-Type method [1]. The small gap between the proposed method and the Newton-Type method is mainly caused by the substitution of two atoms after the refinement step. This action made the accuracy of the TOA and channel amplitude bounded by the accuracy of the AOA and AOD. In other words, our proposed method is a biased estimator for TOA and channel amplitude.

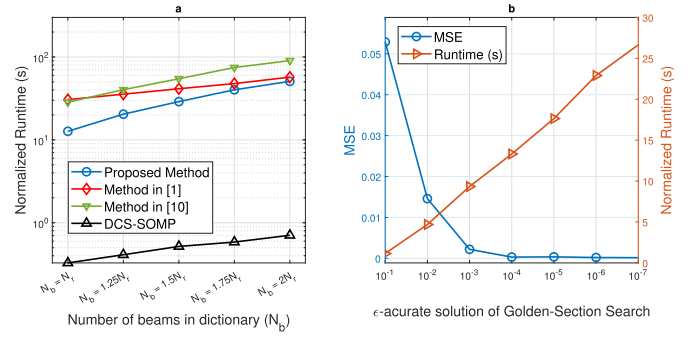


Fig. 4. *a*) Run-time as a function of N_b and *b*) Channel mean square error (MSE) and runtime as functions of tolerance.

B. On the Algorithmic Complexity

Simulation shows that the time complexity of DSC-SOMP is negligible compared to the refinement step, i.e., 2 seconds compared to 20 seconds. The power of the proposed method is concentrated in the refinement step. It mainly involves M_1 times for finding AOD and AOA for K paths. In each loop, it performs a Golden-Section search to find a local minimum. Let ϵ be the tolerance, one step of the Golden-Section then costs $\mathcal{O}(\log(\epsilon^{-1}))$. Each step takes 2 times of evaluating $\tilde{\Omega}$ with size $N_r GN \times N_b N_b N$. Hence, the algorithmic complexity of the refinement step is $\mathcal{O}(2M_1 K(N_r GN \times N_b N_b N) \times \log(\epsilon^{-1}))$. If we use the traditional Newton-type method, the refinement step costs $\mathcal{O}(6M_2 K(N_r GN \times N_b N_b N))$, where M_2 is the number of iterations that must be performed until convergence is achieved. To get a better view of the algorithms' complexity, we measure the running time of methods in two scenarios: *i*) change N_b while fixing the tolerance of Golden-Section search, and *ii*) change the tolerance from 10^{-7} to 10^{-1} while fixing $N_b = N_t$ at a high SNR level. The comparison is shown in Fig. 4. As can be seen in Fig. 4a, our proposed method consumes more computing power than DCS-SOMP and less than methods in [1] and [10]. This can be achieved for two reasons. The first reason is that our proposed method almost has to search on two parameters instead of four, like the Newton-Type method. The second reason can be explained by the fact that the Newton-Type algorithm has to control four descent coefficients without knowing them. This leads to $M_2 > M_1$, i.e., 20–25 compared to 6–8 iterations. From Fig. 4b, we can easily recognize the trade-off of the proposed method. That is, when ϵ decreases, the accuracy of the proposed method increases, but the price we have to pay is the running time. Overall, our refinement method is better than full-dimensional Newton-based search in terms of algorithmic complexity.

V. CONCLUSION

In this letter, we have proposed a novel method for mmWave channel estimation. The idea behind the proposed method is the coordinate descent method with Golden-Section search and DSC-SOMP. We go one step further by proposing a refinement method that reduce the complexity of estimation problems from 4D to almost 2D. The simulation results show that our method provides near the same performance compared

to the Newton-Type algorithm in terms of accuracy with a lower computational cost. We have also shown that the proposed method is biased with respect to TOA and channel gain. Futuristically, we could develop a fully unbiased version with different numerical methods to achieve a lower level of complexity.

APPENDIX: REFINEMENT USING NEWTON-TYPE ALGORITHM

Let $\mathbf{b} = \check{\mathbf{y}} - \sum_{l \neq k, l=0}^K \check{\mathbf{\Omega}} \check{\mathbf{h}}_l^{(i)}$, (16) has the form of LS where $Q = \|\mathbf{b} - \check{\mathbf{\Omega}} \check{\mathbf{h}}_k\|_2^2$. The task normally is to find optimal $\check{\mathbf{h}}_k$ with \mathbf{b} and $\check{\mathbf{\Omega}}$ are known. Since gradient and Hessian of Q is hard to compute, the derivative with respect to single parameter is used instead to sequentially update each one as coordinate descent method. We cyclically update four parameters in $\boldsymbol{\eta}_k = [\eta_{1,k}, \eta_{2,k}, \eta_{3,k}, \eta_{4,k}]^\top = [\theta_{\text{Tx},k}, \theta_{\text{Rx},k}, \tau_k, \tilde{h}_k]^\top$ as follows:

$$\hat{\eta}_{p,k}^{(i+1)} = \hat{\eta}_{p,k}^{(i)} - \gamma_{\eta_{p,k}} \frac{\partial Q}{\partial \eta_{p,k}} \left(\frac{\partial^2 Q}{\partial \eta_{p,k}^2} \right)^{-1}, p = 1, \dots, 4, \quad (21)$$

where, first and second derivative with respect to $\eta_{p,k}$ are defined as

$$\frac{\partial Q}{\partial \eta_{p,k}} = -2 (\mathbf{b} - \check{\mathbf{\Omega}} \check{\mathbf{h}}_k)^H \check{\mathbf{\Omega}} \frac{\partial \check{\mathbf{h}}_k}{\partial \eta_{p,k}}, \quad (22)$$

and

$$\frac{\partial^2 Q}{\partial \eta_{p,k}^2} = 2 \left(\check{\mathbf{\Omega}} \frac{\partial \check{\mathbf{h}}_k}{\partial \eta_{p,k}} \right)^H \left(\check{\mathbf{\Omega}} \frac{\partial \check{\mathbf{h}}_k}{\partial \eta_{p,k}} \right) - 2 (\mathbf{b} - \check{\mathbf{\Omega}} \check{\mathbf{h}}_k)^H \check{\mathbf{\Omega}} \frac{\partial^2 \check{\mathbf{h}}_k}{\partial \eta_{p,k}^2}, \quad (23)$$

respectively. From (11) and $\text{vec} \left(\frac{\partial \check{\mathbf{h}}(\eta_{p,k})}{\partial \eta_{p,k}} \right) = \frac{\partial \text{vec}(\check{\mathbf{h}}(\eta_{p,k}))}{\partial \eta_{p,k}}$, we can obtain the first and second derivative of $\check{\mathbf{h}}_k$ with respect to parameter $\eta_{p,k}$ by the chain rule as follows:

- **AOD:** From (4), the m^{th} element ($m = 0, \dots, N_t - 1$) of the first and second derivation of $\check{\mathbf{h}}_k$ with respect to AOD are reduced to

$$\frac{\partial \mathbf{a}_{\text{Tx},n}^{(m)}(\theta_{\text{Tx}})}{\partial \theta_{\text{Tx}}} = -j\pi m \cos(\theta_{\text{Tx}}) \exp(-j\pi m \sin(\theta_{\text{Tx}})), \quad (24)$$

and

$$\begin{aligned} \frac{\partial^2 \mathbf{a}_{\text{Tx},n}^{(m)}(\theta_{\text{Tx}})}{\partial \theta_{\text{Tx}}^2} &= j\pi m \cos(\theta_{\text{Tx}}) \exp(-j\pi m \sin(\theta_{\text{Tx}})) \\ &\quad \times (j\pi m \cos^2(\theta_{\text{Tx}}) + \sin(\theta_{\text{Tx}})), \end{aligned} \quad (25)$$

respectively.

- **AOA:** Derivatives with respect to AOA are defined the same as AOD by replacing subscript Tx by Rx.

- **TOA:** From (6), the k^{th} element ($k = 0, \dots, K - 1$) of the first and second derivation of $\check{\mathbf{h}}_k$ with respect to TOA are reduced to

$$\frac{\partial \exp \left(\frac{-j2\pi n \tau_k}{NT_s} \right)}{\partial \tau_k} = -j \frac{2\pi n}{NT_s} \exp \left(\frac{-j2\pi n \tau_k}{NT_s} \right), \quad (26)$$

and

$$\frac{\partial^2 \exp \left(\frac{-j2\pi n \tau_k}{NT_s} \right)}{\partial \tau_k^2} = - \left(\frac{2\pi n}{NT_s} \right)^2 \exp \left(\frac{-j2\pi n \tau_k}{NT_s} \right), \quad (27)$$

respectively.

- **Channel Amplitude:** From (6), the k^{th} element ($k = 0, \dots, K - 1$) of the first derivations of $\check{\mathbf{h}}_k$ with respect to channel amplitude is reduced to

$$\frac{\partial |\tilde{h}_k|}{\partial |\tilde{h}_k|} = 1. \quad (28)$$

REFERENCES

- [1] A. Shahmansoori, G. E. Garcia, G. Destino, G. Seco-Granados, and H. Wymeersch, "Position and orientation estimation through millimeter-wave MIMO in 5G systems," *IEEE Trans. Wireless Commun.*, vol. 17, no. 3, pp. 1822–1835, Mar. 2018.
- [2] S. K. Sahoo and A. Makur, "Signal recovery from random measurements via extended orthogonal matching pursuit," *IEEE Trans. Signal Process.*, vol. 63, no. 10, pp. 2572–2581, May 2015.
- [3] R. Mendrik, F. Meyer, G. Bauch, and M. Z. Win, "Enabling situational awareness in millimeter wave massive MIMO systems," *IEEE J. Sel. Topics Signal Process.*, vol. 13, no. 5, pp. 1196–1211, Sep. 2019.
- [4] F. Maschietti, D. Gesbert, P. de Kerret, and H. Wymeersch, "Robust location-aided beam alignment in millimeter wave massive MIMO," in *Proc. IEEE Global Commun. Conf.*, Dec. 2017, pp. 1–6.
- [5] K. Li, M. El-Hajjar, and L.-L. Yang, "Millimeter-wave based localization using a two-stage channel estimation relying on few-bit ADCs," *IEEE Open J. Commun. Soc.*, vol. 2, pp. 1736–1752, 2021.
- [6] S. Srivastava, A. Mishra, A. Rajorija, A. K. Jagannatham, and G. Ascheid, "Quasi-static and time-selective channel estimation for block-sparse millimeter wave hybrid MIMO systems: Sparse Bayesian learning (SBL) based approaches," *IEEE Trans. Signal Process.*, vol. 67, no. 5, pp. 1251–1266, Mar. 2019.
- [7] J. Li, M. F. Da Costa, and U. Mitra, "Joint localization and orientation estimation in millimeter-wave MIMO OFDM systems via atomic norm minimization," *IEEE Trans. Signal Process.*, vol. 70, pp. 4252–4264, 2022.
- [8] R. Zhang, L. Cheng, S. Wang, Y. Lou, W. Wu, and D. W. K. Ng, "Tensor decomposition-based channel estimation for hybrid mmWave massive MIMO in high-mobility scenarios," *IEEE Trans. Commun.*, vol. 70, no. 9, pp. 6325–6340, Sep. 2022.
- [9] J. Du, J. Dong, and F. Gao, "Simultaneous channel estimation and localization of terahertz massive MIMO systems via Bayesian tensor decomposition," *IEEE Commun. Lett.*, vol. 27, no. 2, pp. 541–545, Feb. 2023, doi: 10.1109/LCOMM.2022.3223336.
- [10] N.-S. Duong, T.-M. Dinh-Thi, and Q. T. Nguyen, "mmWave channel estimation for location-based application in 5G MIMO systems," in *Proc. IEEE Region Conf. (TENCON)*, Nov. 2022, pp. 1–6.
- [11] A. A. M. Saleh and R. Valenzuela, "A statistical model for indoor multipath propagation," *IEEE J. Sel. Areas Commun.*, vol. JSAC-5, no. 2, pp. 128–137, Feb. 1987.